WORK OF ADHESION BETWEEN METALS AND POLYMERS ON A MACRO- AND MICROSCOPIC SCALE

M. Füllbrandt[a*], D. Kesal[a], R. v. Klitzing[a]

[a]*Stranski-Laboratorium, Technical University Berlin, Str. d. 17.Juni 124, 10623 Berlin, Germany*
**m.fuellbrandt@tu-berlin.de*

Keywords: Adhesion, Force Measurements, Surface Energy, Roughness

Abstract

Polymer/metal hybrids are of high interest for example in lightweight constructions used in the automotive industry. A fundamental understanding about the adhesion mechanisms at the metal/polymer interface is inevitable. In this contribution the adhesion between different metal/polymer systems is studied on a microscopic scale using atomic force microscopy (AFM) and on a macroscopic scale with contact angle (CA) measurements. With AFM the pull-off force (=adhesive force F_{ad}) between a metal substrate and a polymeric microsphere is determined. The effect of a (sub)micrometer scale roughness on F_{ad} is considered using the Rabinovich approach. With CA measurements the surface energy of the solids is determined using the Owens-Wendt-Rabel-Kaelble (OWRK) method and related to a macroscopic adhesion. Results from both measurements are discussed and correlated.

1. Introduction

Adhesion between polymeric materials and metals plays a major role in many industrial fields, for example, the automotive, aircraft and aerospace industry. The need to join these dissimilar materials is a central challenge. So far the connection between metals and thermoplastics is usually realized by adhesion bonding, screwed fastening or mold-in technique during injection molding.[1] However, a direct adhesive free adhesion is desired. A focus of research is the fundamental understanding of the adhesion mechanism at the polymer/metal interface motivated by the growing needs of the industry for (a) better adhesion properties between polymer and metal components and (b) an improved economical joining process. There are various tests to measure the adhesion including peel-test, lap shear test, torque test, scratch test and pull-off test. [2,3] However, most of the tests are not only destructive but also not suited to obtain any adhesion information on a micro- or even nanoscopic level.

In recent years atomic force microscopy (AFM) has become an important method to measure adhesion forces on a (sub)micrometer scale. Using the colloidal probe (CP) technique introduced in 1991 by Ducker et al.[4] it is possible to make a large variety of probes by attaching all sorts of particles to the cantilever. One of the most important parameter affecting AFM adhesion measurements is surface roughness, a common feature of technical surfaces. Roughness must be taken into account for interpretation of measured AFM adhesion forces

Adhesion studies of technically relevant polymer/metal system using the AFM are rare in literature due to the high complexity of the materials including surface roughness features. For investigations polyamide and polyethylene are chosen as polymer and aluminum and steel as metal component. These technical relevant polymer/metal systems are studied by atomic force microscopy (AFM) and contact angle (CA) measurements. AFM is used for the determination of the pull-off force which corresponds to the adhesive force F_{ad}. The measured F_{ad} values are analyzed using theoretical models of contact mechanics which can relate the force to the work of adhesion W_A. Different models are discussed and the effect of roughness is considered. In order to obtain information on the macroscopic adhesion properties, contact angle (CA) measurements are conducted. The surface energy γ of the polymers and metals is determined using the Owens-Wendt-Rabel-Kaelble method (OWRK).[5,6] From the surface energy the interfacial energy between a given polymer/metal pair can be determined and further be related to the corresponding W_A.

2. Theory and Methods

2.1 Atomic Force Microscopy

Force-Distance Curve: Since 1989 AFM started to become a useful tool for studying surface interaction by means of force-distance curves. The basic concept of atomic force microscopy (AFM) is the measurement of forces between a tip or an attached particle (microsphere) mounted at the end of a cantilever and a sample surface. The technique is well described in literature [7, 8, 9, 10] and not reviewed here. The single steps of a force-distance curve are (a) the tip approach to the sample surface, (b) the jump-to-contact point, where the tip is attracted toward the surface followed by (c) sample indentation or compliance without deformation and (d) cantilever deflection and (e) the retraction of the tip which is hindered by adhesive forces. The so called jump-off contact point is where the tip looses contact to the surface upon overcoming the adhesive forces. A typical force-distance curve measured between a metal substrate and a polyamide microsphere is shown Figure 1.

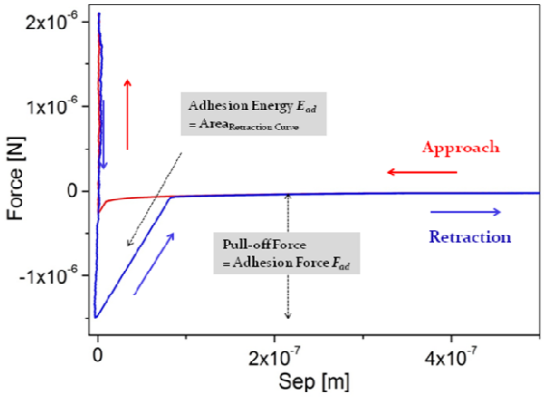

Figure 1: AFM Force-Distance Curve

The product of the jump-off contact cantilever deflection δ_c and the spring constant k_c is the so-called pull-off force and equals the adhesion force F_{ad}. (Hooke's law: $F = -k_c\delta_c$). The adhesion energy E_{ad} can be obtained from the area under the retraction force-distance curve with the baseline taken at zero force but is not discussed in this contribution.

Analysis of adhesion forces*:* The adhesion forces F_{ad} can be quantified by different contact mechanics models. Two models are often used: JKR derived by Johnson et al. [11] in 1971 and DMT derived by Derjaguin et al.[12] in 1975. Both models were derived based on the Hertz theory.[13] More detailed information about these models can be found in literature. The main difference between the two models lies in the assumed nature of forces acting between particle and substrate. For both models the correlation between F_{ad} and W_A is described through a simple analytical equation as follows:

$$F_{ad} = c\pi RW_A \qquad (1)$$

where R is the radius of the particle (microsphere attached to the cantilever) and c is a constant; c=2 for the DMT model and c=1.5 for the JKR model. The JKR and DMT model were developed by assuming a spherical particle in contact with a smooth surface, i.e. two ideal geometries. However, most materials have rough surfaces. Surface roughness at a micro- or nanoscale alters the true contact between the probe and the substrate from that predicted by the contact mechanics models. A model for nanoscale rough surfaces has been proposed by Rabinovich et al.[14]. The Rabinovich model takes the root mean square (rms) roughness parameters along with asperity sizes and distribution into account for a more realistic prediction of the adhesion forces. Rabinovich et al. noticed that many surfaces exhibit two scales of roughness, one is *rms1* associated with a longer peak-to-peak distance λ_1 and a second *rms2* associated with a shorter peak-to-peak distance λ_2. The root-mean square roughness and the peak-to-peak distances can be measured with an AFM in the imaging mode. The Rabinovich model reads:

$$F_{ad} = \frac{c\pi W_A R r_2}{r_2 + R} + \frac{AR}{6H_0^{\,2}} \frac{1}{\left(1 + \frac{58R(rms_1)}{\lambda_1^2}\right)\left(1 + \frac{1.82(rms_2)}{H_0}\right)^2} \qquad (2)$$

where A is the Hamaker constant, R is the radius of the colloidal probe and H_0 is the distance of closest approach between surfaces (approximately 0.3nm). The radius of asperity r_2 and can be replaced by:

$$r_2 = \frac{\lambda_2^{\,2}}{58rms_2} \qquad (3)$$

2.2 Contact angle measurements

Wetting characteristics for a given system can be for example determined using contact angle measurements. Here only the static contact angle θ_c will be considered. In a case of a drop of liquid deposited on a flat, solid surface a meniscus is formed. After spreading a sessile, static drop of the liquid is present. The contact angle θ_c is that between the solid/liquid interface and the tangent to the liquid/air interface as illustrated schematically in Figure 2.

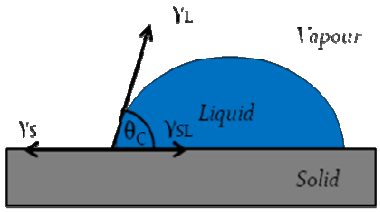

Figure 2: Drop of liquid on a solid substrate. Schematic representation of the static contact angle θ_c. Interfacial tensions are represented by arrows.

The balance between the liquid-vapour, liquid-solid and solid-vapour interfacial tensions determines the capillary forces being related to the contact angle. The mechanical equilibrium fixes the value of the contact angle and one obtains the so called Young Equation [15]:

$$\cos\theta = \frac{\gamma_{SV} - \gamma_{SL}}{\gamma_{LV}} \qquad (4)$$

Wetting is determined by the equilibrium contact angle and can be roughly interpreted as follows: θ_c<90°: good/ partial wetting (hydrophilic surface), θ_c>90°: poor/ no wetting (hydrophobic surface), θ_c = 0°: perfect/ complete wetting.

The work of adhesion W_A is the energy to create two new surfaces from one interface. W_A between two materials (denoted 1 and 2) is given by the Dupré equation [16]:

$$W_{12} = \gamma_1 + \gamma_2 - \gamma_{12} \qquad (5)$$

where γ_1 and γ_2 are the surface free energies of the two materials and γ_{12} is the interfacial energy (interactions) between them.
Using the Fowkes approach [17] the surface energy is a sum of components with a dispersion part *d* and a polar *p* one leading to the following relationship for the interfacial energy between the two phases:

$$\gamma_{12} = \gamma_1 + \gamma_2 - 2\left(\sqrt{\gamma_1^d \gamma_2^d} + \sqrt{\gamma_1^p \gamma_2^p}\right) \qquad (6)$$

The surface tension of a solid (S) with its polar and dispersive part can be experimentally determined by measuring the contact angle with a series of probe liquids (L) with known surface tension γ_L, including $\gamma_L{}^d$ and $\gamma_L{}^p$. For calculation of the surface energy of the solid the Owens-Wendt-Rabel-Kaelble plot (OWRK) [18, 19] is used.

3. Materials and Experimental

3.1 Polymeric microspheres

Polymeric microspheres made of Polyamide 6 (PA6) and Polyethylene (PE) are used for AFM measurements. They have a diameter between 10 and 20 µm . Microspheres were glued with epoxy to a tipless cantilever with a given spring constant of 5.4 to 17 N/m (NSC35 Mikromasch). Microsphers are characterized by scanning electron microscopy (SEM) and an

optical microscope. Images of an exemplary PA6 microsphere attached to a cantilever are presented in Figure 3.

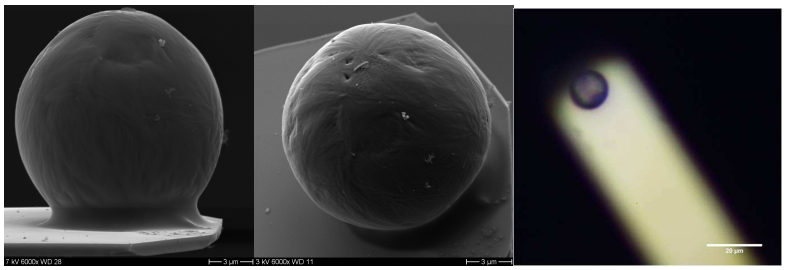

Figure 3: *Left and middle image*: SEM images of a PA6 microsphere coated with a 5 nm carbon layer attached to a cantilever, side and top view. *Right image*: Optical microscope image of the same PA6 microsphere.

3.2 Metal substrates

As metal substrates an aluminum alloy (AlMg4,5Mn0,4) and a dual phase steel were used referred to in the following as Al and DPS sample, respectively. Technical surfaces exhibit a quite rough surface (micrometer range) not suitable for AFM and CA investigations. Therefore prior to measurements Al and DPS samples were mechanically polished in order to obtain a rather smooth surface with nm scaled roughness (see Figure 4).

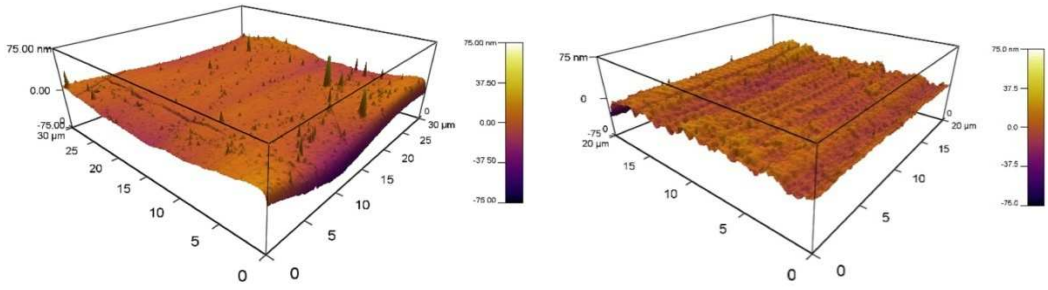

Figure 4: 3D AFM images of a polished Al sample (left image) and a DPS sample (right image).

3.3 Experimental

Force-separation curves are collected with an atomic force microscope MFP3D (Asylum Research, Inc.). Measurements are conducted in a dry nitrogen atmosphere at 30 °C using a cell that can be fully sealed with a membrane and operated in a wide temperature range. The humidity was kept under RH 5 % throughout the whole measurement. Statistical data evaluation is needed for a proper interpretation of the adhesion force. One measurement set consisted of around 5 to 8 force maps collected at different locations of the sample. One force map includes 100 single force curves obtained over an area of 90 x 90 µm. The applied load was kept constant with 2000 nN. Measurements were repeated several times in order to check reproducibility. An adhesion histogram was generated from the results and mean and standard deviation were calculated by fitting a Gaussian distribution to the histogram.

Contact angle measurements are performed by the sessile drop method. The contact angles were measured with a Goniometer OCA20 (Dataphysics, Germany). The solid samples are placed on a sample stage in a closed cell which is filled by one third with the respective measuring liquid in order to obtain a saturated atmosphere. Samples are equilibrated for around 30 min before a drop of the liquid is placed on the surface via a syringe. A video was

recorded for 90 min and the software SCA 20 determined the contact angle using the Young-Laplace fitting method. Three to four different liquids were used for each solid substrate. Per liquid 3 drops were placed on different spots of the substrate and the equilibrium contact angle was averaged over the three measurements.

4. Results and Discussion

4.1 Adhesion on a macroscopic scale determined by CA measurements

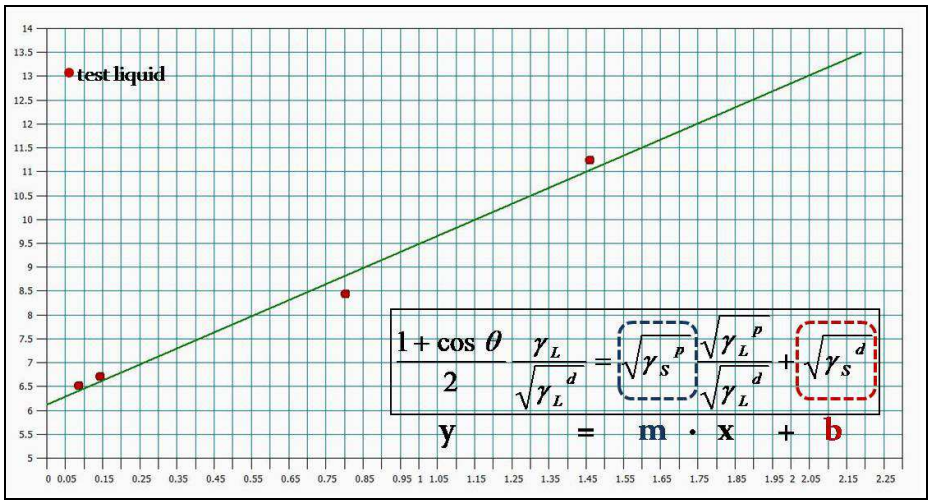

Figure 5: OWRK plot for PA6.

The surface energies of PA6, Al and DPS with polar and dispersive part are listed in Table 1. The values are obtained from the corresponding OWRK plot. An example is shown in Figure 5 with the corresponding equation. Results are comparable with literature values.

Sample	*Surface energy γ [mN/m]*	*Dispersive part γ^d [mN/m]*	*Polar part γ^p [mN/m]*
Al	48.3	30.7	17.6
DPS	40.9	31.2	9.7
PA6	42.3	37.1	5.2

Table 1: Surface energies determined from the OWRK plot.

Using the surface energy of each component, the interfacial energy and the work of adhesion is calculated for PA6/Al and PA6/DPS. Results are summarized in Table 2.

Sample pair: Metal/Polymer	*Interfacial energy γ_{12} [mN/m]*	*Work of Adhesion W_{12} [mN/m]*
PA6/ Al	1.0	82.2
PA6/ DPS	4.0	86.6

Table 2: Interfacial energy and work of adhesion for PA6/Al and PA6/DPS.

4.2. Adhesion on a microscopic scale determined by AFM force measurements

The adhesion force measured between Al/PA6 and DPS/PA6 is presented in Figure 6. Each measurement consists of 1000-1300 single force plots collected on two different days from two different samples of the same metal. The microsphere was not changed within one measurement. Data are fitted with a Gaussian curve and the mean force values are normalized to the radius of the sphere for better comparison.

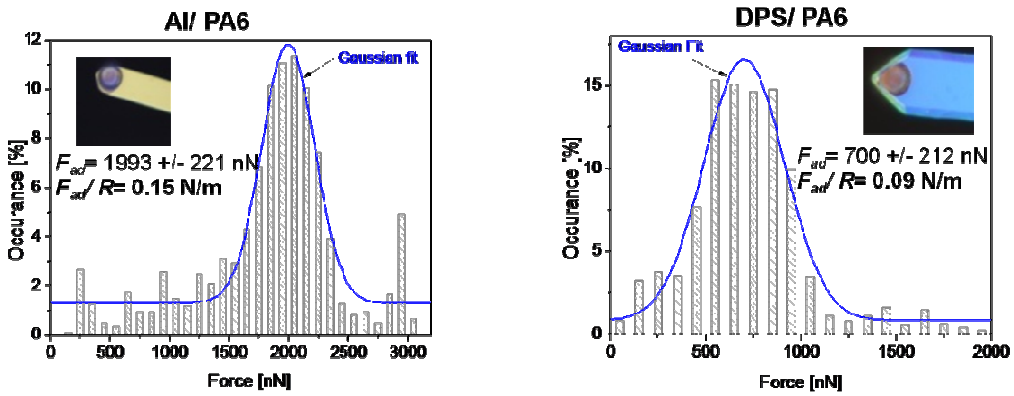

Figure 6: Adhesion force between Al/PA6 (left image) and DPS/PA6 (right image).

As discussed in the theory part, adhesion forces can now further be related to the work of adhesion using different models. Results for the JKR, DMT and Rabinovich model are given in Table 3.

Model	*W_A [mN/m] Al/ PA6*	*W_A [mN/m] DPS/ PA6*
JKR	33	19
DMT	24	14
Rabinovich	84	78

Table 3: Work of Adhesion according to JKR, DMT and Rabinovich model.

Using the JKR or DMT model leads to quite small W_A values compared to the Rabinovich model. The reason is that for the JKR and DMT model the surface roughness is not considered. Therefore a wrong contact area is assumed leading to an underestimation of W_A. The Rabinovich model leads to higher W_A values which are actually in the same region than the macroscopic W_A values (see Table 2). The work of adhesion between DPS/PA6 seems to be slightly smaller than for Al/PA6. A finding which is not supported from the CA measurements. Further measurements are necessary for a final conclusion.

5. Conclusion

The adhesion between PA6 and metal samples (Al, DPS) on different length scales was measured. The adhesion properties on a macroscopic scale were determined from contact angle measurements. The adhesion force on a micro- or even nanoscopic scale was obtained from AFM force measurements. The method required a careful analysis of the surface roughness of the metal samples in order to predict a realistic contact area. However, it was shown that if considering the roughness characteristics of the substrate a work of adhesion similar to the macroscopic one was obtained. A more careful analysis of the different

adhesion contributions is required. In a next step measurements with (a) varying the polymer component and (b) the metal surface are planned

References

[1] M. Grujicic; V. Sellappan; M.A. Omar; N. Seyr; A. Obieglo; M. Erdmann; J. Holzleitner. *J Mater Process Tech*, 197: 363-373, 2008.
[2] F. Awaja; M. Gilbert; G. Kelly; B. Fox; P. Pigram. *J. Progress In Polymer Science*, 34: 948-968, 2009.
[3] A.L. Gasparin; C.H. Wanke; R.C.R. Nunes; E.K. Tentardini; C.A. Figueroa; I.J.R. Baumvol; R.V.B. Oliveira. *Thin Solid Films*, 534: 356-362, 2013.
[4] W. Ducker; T. Senden; R. Pashley. *Nature*, 353: 239-241, 1991.
[5] D.K. Owens; R.C. Wendt. *J. Appl. Polym. Sci.*, 13: 1741,1969.
[6] D.H. Kaelble. *J. Adhes.*, 2: 66, 1970.
[7] B. Cappella; G. Dietler. *Surf. Sci. Rep.*, 34: 1, 1999.
[8] D. Sarid (Ed.) *Scanning Force Microscopy;* Oxford Univ. Press, Cambridge, 1991.
[9] H.J. Butt; B. Cappella; M. Kappl *Surf. Sci. Rep.*, 59: 1-152, 2005.
[10] R. Wiesendanger (Ed.) *Scanning Probe Microscopy and Spectroscopy: Methods and Applications*; Oxford Univ. Press, Cambridge, 1994.
[11] K.L. Johnson; K. Kendall; A.D. Roberts *Proceedings of the Royal Society of London Series A-mathematical and Physical Sciences*, 324: 301, 1971.
[12] B. Derjaguin; V.M. Muller; Y.P. Toporov. *J. Colloid Interface Sci.*, 314-326: 53, 1975.
[13] H. Hertz, *Miscellaneous Papers*; Macmillan, London, 1896.
[14] (a) Y.I. Rabinovich; J.J. Adler; A. Ata; R.K. Singh; B.M. Moudgil. *J. Colloid Interface Sci.*, 232: 10-16, 2000. (b) (a) Y.I. Rabinovich; J.J. Adler; A. Ata; R.K. Singh; B.M. Moudgil. *J. Colloid Interface Sci.*, 232: 17-24, 2000.
[15] T. Young *Philos. Trans. R. Soc.*, 95: 65-87, 1805.
[16] A. Dupré, A. *Théorie mécanique de la chaleur*; Paris: Gauthier-Villars, 1869.
[17] F.M. Fowkes. *J. Phys. Chem.*, 67: 2538-2541, 1963.
[18] D.K.Owens; R.C. Wendt . *J. Appl. Polym. Sci.*, 13: 1741,1969.
[19] D.H. Kaelble. *J. Adhes.*, 2: 66, 1970.